

# Charpy Impact of Sandwich Structural Composites (CFRP/PC/CFRP) of Polycarbonate (PC) Cores Covered with Carbon Fiber Cross Textile Reinforced Epoxy Polymer (CFRP) Thin Sheets as a Function of Temperature

Yoshitake Nishi<sup>1</sup>, Naoya Tsuchikura<sup>1,\*</sup>, Shinichiro Nanba<sup>1,\*</sup>,  
Tatsuya Yamamoto<sup>1,\*</sup> and Michael C. Faudree<sup>1,2</sup>

<sup>1</sup>Department of Metallurgical Engineering, Graduate School of Engineering, Tokai University, Hiratsuka 259-1292, Japan

<sup>2</sup>Center of Foreign Language, Tokai University, Hiratsuka 259-1292, Japan

The purpose of this study is to investigate a lighter, cheaper and possibly stronger alternative to CFRP, by obtaining the Charpy impact values ( $a_{uc}$ ) of a sandwich structural composite (CFRP/PC/CFRP) constructed of a polycarbonate (PC) core between two thin plies of carbon cross textile fiber/epoxy (CFRP) within the temperature range of aircraft operation, from 200 to 403 K below the glass transition temperature of PC ( $T_g = 422$  K). The  $a_{uc}$  of CFRP/PC/CFRP were compared with a 2.0 mm thick 12-ply CFRP laminate. Results showed overall, the CFRP/PC/CFRP had higher  $a_{uc}$  than the CFRP at each fracture probability ( $P_f$ ) from 300 to 373 K except at 200 K with low  $P_f$  and 403 K with high  $P_f$ . Specifically, although the volume fraction of carbon fiber (12%) of CFRP/PC/CFRP was much smaller than that (60%) of the CFRP, the  $a_{uc}$  at room temperature (300 K) of CFRP/PC/CFRP was approximately 64% higher than that of CFRP at mid-fracture probability ( $P_f$ ) of 0.50. Fracture modes of CFRP/PC/CFRP were explained by delamination between PC core and the CFRP thin sheet surfaces, bending plastic deformation, and CFRP fracture. The highest Weibull coefficient ( $n$ ) was obtained at 323 K. Based on the 3-parameter Weibull equation, the limiting impact value ( $a_c$ ) also exhibited the highest value at 323 K. In addition, the cost of CFRP/PC/CFRP was 40% lower than that of CFRP at the time of this study. Since the use of PC resin as the core enhanced the safety design at low cost, practical use of sandwich structural composites of CFRP/PC/CFRP is possible. [doi:10.2320/matertrans.M2011357]

(Received December 8, 2011; Accepted April 9, 2012; Published May 30, 2012)

**Keywords:** sandwich structure, carbon fiber reinforced polymer (CFRP), epoxy, polycarbonate, Charpy impact test, delamination

## 1. Introduction

Carbon fiber reinforced polymer (CFRP) has been utilized for light structural materials with high strength.<sup>1,2)</sup> The further strengthening with safety enhancement has been always expected to develop high-speed transport vehicles with safety and low energy consumption. However, the high strength carbon fiber, whose supply often cannot catch up with demand exhibits a high cost.

On the other hand, sandwich panels made with laminate skins and light-weight cores are commonly employed in the aerospace, marine, automotive and recreational industries. With their superior bending stiffness, low weight, good thermal insulation, acoustic damping, ease of machining and high corrosion resistance sandwich panels exhibit advantages over metallic materials. Conversely, limitations include possible low interlaminar shear strength and susceptibility to impact damage, especially between the core and face sheets.

Traditionally, damage by a hemispherical impactor is initiated as a point force on the center of a square or rectangular specimen  $\sim 70$  to  $150 \text{ mm}^2$  by slow point force,<sup>3)</sup> drop tower, or projectile.<sup>4-7)</sup> For low energy tests, impact is followed by non-destructive testing (NDT) with an ultrasonic transducer to detect delamination undetectable to the eye which can reduce strength significantly. Compression after impact (CAI) testing is often conducted after point impact in aerospace materials such as quasiisotropic CFRP for safety design.<sup>8,9)</sup>

Five fracture modes in composite laminates and sandwich panels undergoing point impact have been identified: core

crushing, core cracking, delamination in the impacted face sheet, matrix cracking, and fiber breakage in the face sheets.<sup>10)</sup> This method of point impact fracture followed by CAI for aircraft CFRP has been generally studied to evaluate safety against impact accidents such as bird strike, volcanic rock or hailstone on aircraft CFRP.<sup>11,12)</sup>

On the other hand, the Charpy impact test utilizes a drop-weight pendulum and evaluates the impact absorption characteristics and relative impact toughness of materials often used in quality control applications employed as an inexpensive and fast way to estimate reaction to higher velocity impact. We do not claim the Charpy test to be a substitute for point impact followed by compression after impact (CAI). However, Charpy impact method could possibly be used as an inexpensive preliminary evaluation to screen candidate materials to later test with indentation or projectile followed by CAI. Hence, Charpy may give a rough or better estimation of which materials and what temperatures a projectile such as bird strike, volcanic rock or hailstone will cause the most damage. Tests are carried out calibrating for air friction and effect of air temperature and humidity on the swing and pivot of the pendulum. Therefore the velocity,  $v$  ( $\text{m s}^{-1}$ ) and kinetic energy,  $KE$  (J) hitting the sample are assumed to be approximately constant similar to comparing projectiles in a point impact test hitting the composite surface at constant  $v$  and  $KE$ . Thus, when the Charpy impact test impact velocity,  $v$  hitting the sample is calculated as:<sup>13)</sup>

$$v = [2gR(1 - \cos \alpha)]^{0.5} \quad (1)$$

where  $g$  is gravitational constant ( $9.8 \text{ m s}^{-2}$ ),  $R$  is length (m) of hammer weight point from rolling center (0.21 m), and  $\alpha$  is start angle before impact ( $2.3$  Radians,  $132^\circ$ ), then  $v$  of the

\*Graduate Student, Tokai University

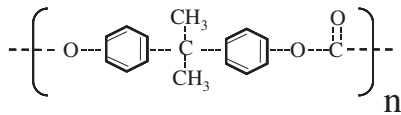


Fig. 1 Structural formula of polycarbonate.

hammer hitting the specimen is  $\sim 1.74 \text{ m s}^{-1}$  ( $\sim 3.89 \text{ mi/hr}$ ). Potential energy ( $PE$ ) (J) of impact is:<sup>13)</sup>

$$PE = R(1 - \cos \alpha)F \quad (2)$$

where  $F$  is the measured supporting force (N) exerted by the pendulum in the horizontal position.  $PE$  is assumed to be equivalent to the  $KE$  in the horizontal vector,  $0.5mv^2$ , or  $1.30 \text{ J}$  ( $1.3 \times 10^{-3} \text{ kJ}$ ). The surface area of the impactor is small so  $KE/A$  is large.

It follows to reduce cost and increase safety compared to the CFRP, sandwich structural composites (CFRP/ABS/CFRP and CFRP/PMMA/CFRP) of both acrylonitrile butadiene styrene (ABS) and poly methyl methacrylate (PMMA) resins cores covered with carbon fiber reinforced polymer (CFRP) sheets at both side surfaces have been suggested because of crack generation prevention near the surface.<sup>14)</sup> The impact value,  $a_{uc}$  of CFRP/ABS/CFRP,<sup>14)</sup> which approximately corresponds to that of CFRP composite,<sup>15)</sup> is more than two times higher than that of CFRP/PMMA/CFRP.<sup>14)</sup> In addition, since the price of CFRP is higher than that of ABS resin, the sandwich structural composites of CFRP/ABS/CFRP cost only 20% that of CFRP, hence practical use is possible.

Although the price (13,700 Yen/ $1.0 \text{ mm} \times 1.0 \text{ mm} \times 2.0 \text{ mm}$  in 2011 Feb. Tokyo) of high strength polycarbonate (PC) was higher than that of ABS resin (6240 Yen/ $1.0 \text{ mm} \times 1.0 \text{ mm} \times 2.0 \text{ mm}$  in 2011 Feb. Tokyo), the benefits are PC exhibits high heat resistance ( $T_g = 422 \text{ K}$ ),<sup>16)</sup> low flammability,<sup>17)</sup> high elasticity, 2.1 to 2.4 GPa<sup>18)</sup> and high  $a_{uc}$  ( $84 \text{ kJ m}^{-2}$ ).<sup>19)</sup> Figure 1 shows the structural formula of PC with its two hexagonal hard segments in one monomer. Thus, the high strength of sandwich structural composites of CFRP/PC/CFRP can be expected.

Up to now, there has been no or very little research on Charpy impact value ( $a_{uc}$ ) of composite sandwich structures. It is very important to evaluate the safety against impact accidents such as flying volcanic debris and hailstorms, as well as bird strike, volcanic rock or hailstone.<sup>20,21)</sup> The applied temperature range of airplane CFRP is generally from more than 200 to less than 400 K. Thus, the purpose of this study is to investigate a cheaper and possibly stronger alternative to CFRP, by obtaining the Charpy impact values of a sandwich structural composite constructed of a polycarbonate (PC) core between two thin plies of carbon cross textile fiber/epoxy (CFRP/PC/CFRP) within the temperature range of aircraft operation, from 200 to 403 K.

## 2. Experimental Procedure

### 2.1 Sample preparation

As shown in Fig. 2, the volume of sandwich structural composites of CFRP/PC/CFRP of PC core (Takiron Ltd., Tokyo) covered with carbon fiber cross textile reinforced

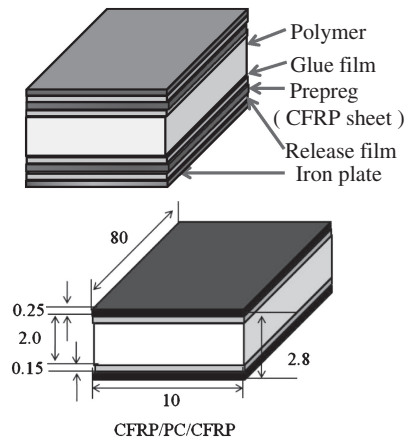


Fig. 2 Schematic diagram of sandwich structural composite of CFRP/PC/CFRP.

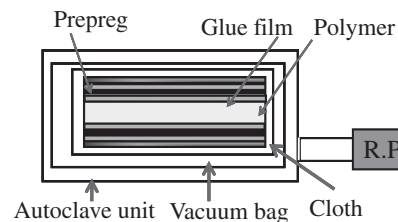


Fig. 3 Schematic diagram of autoclave unit.

epoxy thin sheets at both side surfaces (CFRP, 0.25 mm thickness, TR3110-331MP epoxy/CF, Mitsubishi Rayon Ltd., Tokyo) was  $2240 \text{ mm}^3$ . Since adhesive force between PC and CFRP is not high, glue film (NB-102HC-50-0.06, GH-Craft Ltd., Tokyo) was used to make the composites.

As shown in Fig. 3, the CFRP/PC/CFRP laminate sample was pre-preged. Volume fraction,  $V_f$  of carbon fiber and PC core were 12 and 88 vol%, respectively. In the CFRP sheet,  $V_f$  of carbon fiber was 60%. Making composites was performed by autoclave molding in vacuum under 1 Pa for 2 h at 403 K.

Since the bundle direction was the longitudinal direction, a high unidirectional strength perpendicular to the sheet plane can be expected.

### 2.2 Impact test and its condition at high and low temperatures

In order to evaluate the impact fracture toughness, the Charpy impact values of the CFRP/PC/CFRP and CFRP samples with and without heating and cooling were measured using a standard impact fracture energy measurement system (Shimadzu Corporation No. 51735) (JIS K 7077).<sup>22)</sup> CFRP sample sizes were a 12-ply laminate with dimensions  $80 \times 10 \times 2.0 \text{ mm}$ . The impact fracture energy ( $E$ ) was expressed by the following equation.<sup>22-26)</sup>

$$E = WR[(\cos \beta - \cos \alpha) - (\cos \alpha' - \cos \alpha)(\alpha + \beta)/(\alpha + \alpha')] \quad (3)$$

Here,  $E$ ,  $W$ ,  $R$ ,  $\beta$ ,  $\alpha$  and  $\alpha'$  were impact fracture energy (J), hammer weight (8.43 N), length (m) of hammer weight point from rolling center (0.21 m), the maximum angle after impact, start angle before impact ( $132^\circ$ ), and the maximum

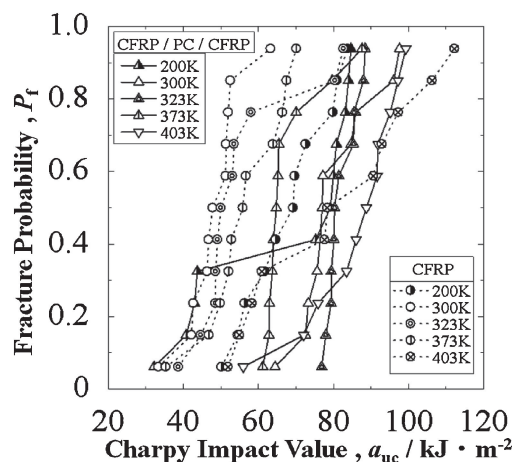


Fig. 4 Changes in Charpy impact value ( $a_{uc}$ ) of CFRP/PC/CFRP (solid lines) at each temperature against fracture probability ( $P_f$ ), together with CFRP (dotted lines).

angle of the blank test (Radians), respectively. The Charpy impact value ( $a_{uc}$ :  $\text{kJ m}^{-2}$ ) was expressed by the following equation.<sup>22)</sup>

$$a_{uc} = E/(bt) \times 10^3 \quad (4)$$

Here,  $E$ ,  $b$  ( $= 10 \pm 0.2$  mm) and  $t$  ( $= 2.8$  mm) were impact fracture energy (J), sample width (mm) and span distance (sample thickness, mm), respectively. The distance between supporting points was 40 mm.

The samples were cooled by liquid nitrogen and ethanol with dry ice and heated by heat gun (brawler). The impact test was performed, when the sample temperature was constant.

### 3. Results

#### 3.1 Impact values of CFRP/PC/CFRP

Impact values ( $a_{uc}$ ) of sandwich structural composites (CFRP/PC/CFRP) of polycarbonate (PC) cores covered with thin sheets of carbon fiber cross textile reinforced epoxy (CFRP) at both side surfaces have been obtained. Figure 4 shows changes in Charpy impact value of CFRP/PC/CFRP against fracture probability ( $P_f$ ) at each testing temperature from 200 to 403 K below the glass transition temperature of PC ( $T_g = 422$  K)<sup>16)</sup> and epoxy ( $T_g = 403$  K).

Results show overall, the CFRP/PC/CFRP has higher  $a_{uc}$  values than the CFRP. Note Fig. 4 shows the  $a_{uc}$  at room temperature (300 K) of CFRP/PC/CFRP ( $77 \text{ kJ m}^{-2}$ ) is approximately 64% higher than that of CFRP sheet ( $47 \text{ kJ m}^{-2}$ ) at mid- $P_f$  of 0.50. Moreover, the  $a_{uc}$  values of CFRP/PC/CFRP at all fracture probabilities ( $P_f$ ) at 300, 323 and 373 K as well as mid- $P_f$  of 0.50 at each temperature from 200 to 403 K are apparently higher than that of the CFRP. Although  $a_{uc}$  the CFRP/PC/CFRP is reduced below the CFRP for 200 and 403 K below  $P_f = 0.40$  and above  $P_f = 0.60$  to 0.70, respectively,  $a_{uc}$  of the CFRP/PC/CFRP improves over the CFRP at  $a_{uc}$  above  $P_f = 0.40$  and below  $P_f = 0.60$  to 0.70, respectively. Both the CFRP/PC/CFRP, and CFRP sheet have the highest  $a_{uc}$  at 403 K.

The  $a_{uc}$  of CFRP/PC/CFRP heated at water boiling point of 373 K is always lower than that at 300 K at each  $P_f$  value from 0.12 to 0.94; at 323 K the  $a_{uc}$  values at lower  $P_f$  from

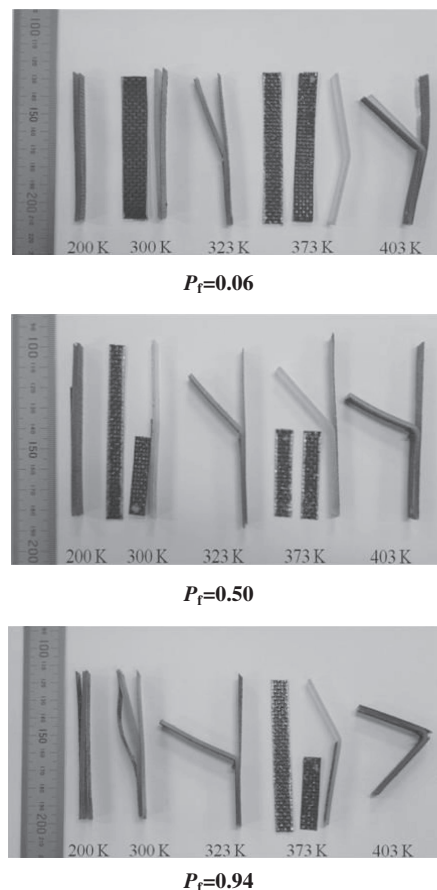


Fig. 5 Photographs of fractured CFRP/PC/CFRP sandwich structures at each testing temperature at low, mid- and high  $P_f$ .

0.06 to 0.78 of CFRP/PC/CFRP are mostly higher than that at 300 K. At 403 K all  $a_{uc}$  values between  $P_f$  from 0.12 to 0.94 of CFRP/PC/CFRP are higher than that at 300 K.

When the CFRP/PC/CFRP sample is cooled at nitrogen boiling point of 77 K, delamination occurs before the impact test. Thus,  $a_{uc}$  cannot be obtained at 77 K.

The higher  $a_{uc}$  of CFRP/PC/CFRP at 200 K is found from 77 to  $83 \text{ kJ m}^{-2}$  at higher  $P_f$  of more than 0.41, whereas the lower  $a_{uc}$  of CFRP/PC/CFRP at 200 K is distributed from 32 to  $42 \text{ kJ m}^{-2}$  at lower  $P_f$  of less than 0.41. The  $a_{uc}$  of CFRP/PC/CFRP cooled at low temperature of 200 K is higher than that at 300 K at mid- $P_f$  values of 0.50 and 0.59, although it is lower than that at low and high  $P_f$  values of less than 0.41 and more than 0.58, respectively.

#### 3.2 Optical observation of fractured CFRP/PC/CFRP at each testing temperature

Figure 5 shows photographs of fractured CFRP/PC/CFRP samples at the testing temperatures from 200 to 403 K showing fracture occurred with delamination of surface CFRP thin sheets within the total  $P_f$  range.

Note fracture cannot be observed in the PC core at all testing temperatures. Heating from 323 to 403 K results in remarkable bending plastic deformation of the core, whereas cooling from 300 to 200 K results in bending elastic deformation of the core at each  $P_f$ .

Fracture and/or surface damage of impacted CFRP sheets occur at mid- $P_f$  of 0.50 from 200 to 403 K; at mid- and high

Table 1 Fracture mode, impact value ( $\text{kJ m}^{-2}$ ) and reduced delamination area against sheet sample area at low, mid- and high fracture probability ( $P_f = 0.06, 0.50$  and  $0.94$ ) at each impact test temperature of 200, 300, 323, 373 and 403 K, respectively.  $\triangle$  and  $\nabla$  are delamination at CFRP sheets at impact side and tensile sides, respectively. Solid and half solid triangles are fractured and damaged CFRP by impact test, respectively.  $\textcircled{1}$  and  $\textcircled{0}$  are PC core with and without bending plastic deformation, respectively.  $\square$  is the delamination fracture site.

$P_f$	Impact test temperature				
	200	300	323	373	403
0.06	$\triangle\textcircled{0}\square\nabla$ 32.2 (0.5)	$\triangle\textcircled{0}\square\nabla$ 64.4 (1.0)	$\triangle\textcircled{1}\square\nabla$ 76.9 (0.5)	$\triangle\textcircled{0}\square\nabla$ 61.2 (2.0)	$\triangle\textcircled{1}\square\nabla$ 56.0 (0.5)
0.50	$\blacktriangle\textcircled{0}\square\nabla$ 79.2 (0.5)	$\blacktriangle\textcircled{0}\square\nabla$ 77.0 (1.5)	$\blacktriangle\textcircled{1}\square\nabla$ 80.3 (0.5)	$\blacktriangle\textcircled{0}\square\nabla$ 64.8 (1.0)	$\blacktriangle\textcircled{1}\square\nabla$ 88.8 (0.5)
0.94	$\triangle\textcircled{0}\square\nabla$ 84.6 (1.0)	$\triangle\textcircled{0}\square\nabla$ 97.6 (1.0)	$\triangle\textcircled{1}\square\nabla$ 88.4 (0.5)	$\blacktriangle\textcircled{0}\square\nabla$ 87.6 (1.5)	$\blacktriangle\textcircled{1}\nabla$ 99.3 (0.0)

$P_f$  at 373 K; and at each  $P_f$  at 323 and 403 K; although fracture of the CFRP thin sheet at the tensile surface side of the sample heated at 403 K occurs at high  $P_f$  of 0.94. Both PC core bending plastic deformation and delamination between core and CFRP sheet at impacted and tensile sides are found in the sample of each  $P_f$  heated at 373 K.

## 4. Discussion

### 4.1 Fracture mode dependent impact value

Up to now, there has been no or very little research on Charpy impact value ( $a_{uc}$ ) of composite sandwich structures. However, there is extensive research on point impact<sup>3–11</sup> and point impact followed by CAI<sup>8,9</sup> to evaluate strength of damaged aerospace materials. Point impact followed by CAI is very different than Charpy impact. In Charpy impact, a thin specimen (Fig. 5) is impacted across its entire cross-section, whereas in point impact the center of a wider specimen is impacted from a point source. Since Charpy is an easy and economical method, we will compare fracture modes of this study with those of point impact mentioned previously: core crushing, core cracking, delamination in the impacted face sheet, matrix cracking, and fiber breakage in the face sheets.<sup>10</sup> Different than point impact, Charpy impacted specimens in Table 1 show no evidence of core crushing or cracking, and no delamination within the impacted face sheet since it is only one ply. Similar to point impact, there appears to be matrix cracking and fiber breakage from the Charpy impact tests.

Specifically, based on the results in Figs. 4 and 5, the fracture mode, impact value ( $\text{kJ m}^{-2}$ ) and reduced delamination area against sheet sample area at low, mid- and high fracture probability ( $P_f = 0.06, 0.50$  and  $0.94$ ) at each impact test temperature of 200, 300, 323, 373 and 403 K are summarized in Table 1. Fracture mode is explained by a delamination between PC core and surface CFRP thin sheets, bending plastic deformation of the PC core and CFRP fracture. Table 1 and Fig. 5 show the PC is a strong core because there is no evidence of core crushing or cracking. However overall, there is delamination in the impacted and back face sheets indicating a stronger bonding agent would probably increase  $a_{uc}$  further.

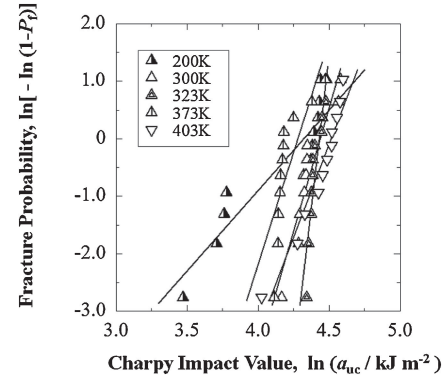


Fig. 6 Weibull plots of CFRP/PC/CFRP at each temperature.

Although the CFRP thin sheet fracture at tensile surface side occurs with negligible delamination area, the bending plastic deformation of the PC core of the sample with the highest  $a_{uc}$  ( $99.3 \text{ kJ m}^{-2}$  at high  $P_f$  of 0.94 under the highest test temperature of 403 K in Table 1) occurs. The plastic deformation of PC is one of the dominant factors to relax the impact energy.

On the contrary, the sample with 2nd highest  $a_{uc}$  ( $97.6 \text{ kJ m}^{-2}$  at high  $P_f$  of 0.94 at room temperature of 300 K in Table 1) exhibits the delamination fracture at both interfaces between elastic deformed PC core and CFRP sheets (see Table 1). The delamination is also one of the dominant factors to relax the impact energy.

### 4.2 Weibull coefficient ( $n$ ) of CFRP/PC/CFRP

The Weibull coefficient ( $n$ ) is one of the standard and traditional factors to compare with many other structural materials.<sup>22–25</sup> When  $a_{uc}$  is the measured Charpy impact value and a constant, the fracture probability ( $P_f$ ) as a function of the risk of rupture ( $a_{uc}/a_o$ ) is expressed by the following equation.<sup>26</sup>

$$P_f = 1 - \exp[-(a_{uc}/a_o)^n] \quad (5)$$

The linear relationship can be obtained as the following equation.

$$\ln(-\ln(1 - P_f)) = n \ln a_{uc} - n \ln a_o \quad (6)$$

Figure 6 shows Weibull plots of CFRP/PC/CFRP at each temperature. The  $n$  value corresponds to the slopes of the relationships of Weibull plots.

Figure 7 shows the change in Weibull coefficient,  $n$  of CFRP/PC/CFRP against testing temperature. The high  $n$  values, which are higher than those at high and low temperatures of 200 and 403 K, are obtained from 300 to 373 K. The highest  $n$  value of 22 related to reliability with low experimental error of CFRP/PC/CFRP is obtained at 323 K.

### 4.3 Temperature dependent lowest impact value of CFRP/PC/CFRP

On the other hand, since the experimental impact values at lower  $P_f$  value have largely deviated from the linear relationship (see Fig. 4), the practical impact value at low  $P_f$  value cannot be estimated.



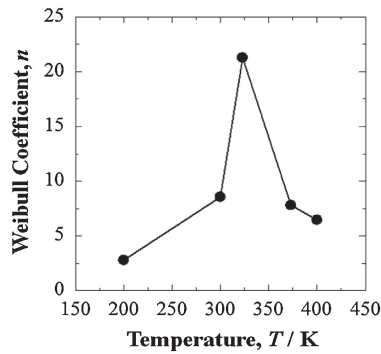


Fig. 7 Changes in Weibull coefficient of CFRP/PC/CFRP at each temperature.

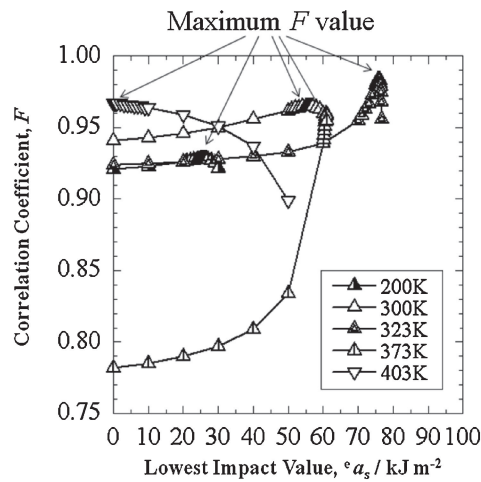


Fig. 8 Changes in the  $F$  value of CFRP/PC/CFRP with respect to the  $a_s$  value.

If the statistical equation is assumed to be applicable to the measured  $a_{uc}$  value, the  $P_f$  value depends on the risk of rupture ( $[a_{uc} - a_s]/a_{III}$ ).<sup>22-25,27)</sup>

$$P_f = 1 - \exp[-([a_{uc} - a_s]/a_{III})^m] \quad (7)$$

In predicting the required impact value of the new structural material, the lowest impact value ( $a_s$ ), the coefficient ( $m$ ) and constant ( $a_{III}$ ) are key parameters. The  $a_{III}$  is the  $a_{uc}$  value at  $P_f$  of 0.632 when the term ( $\ln[-\ln(1 - P_f)]$ ) is zero.

When the  $P_f$  value is equal to zero, the  $a_{uc}$  value is defined as the  $a_s$  value. When a correlation coefficient ( $F$ ) of eq. (5) shows the maximum value, the potential ( $a_s$ ) value can be determined to be the lowest impact value ( $a_s$ ) applied. Figure 8 shows changes in the  $F$  value with respect to the  $a_s$  value. Since the  $F$  values are from 0.92 to 0.97 in Fig. 8, the relationships in Fig. 9 exhibit the high linearity. Figure 9 shows linear relationships between  $\ln(a_{uc} - a_s)$  and  $\ln[-\ln(1 - P_f)]$  for CFRP/PC/CFRP at each temperature. The values of  $a_{III}$  and  $m$  are determined by the least squares best fit method. The  $m$  value is estimated by the slope of the relationship as a function of the  $a_s$  value. Figure 10 shows changes in experimental impact values ( $a_{uc}$ ) at low  $P_f$  of 0.06 ( $\circ$ ) and the lowest impact values ( $\bullet$ :  $a_s = a_{uc}$  at  $P_f = 0$ ) of CFRP/PC/CFRP plotted against temperature. Based on the results, the high  $a_s$  values, which are higher than those (27 and zero kJ m<sup>-2</sup>) at high and low temperatures of 200

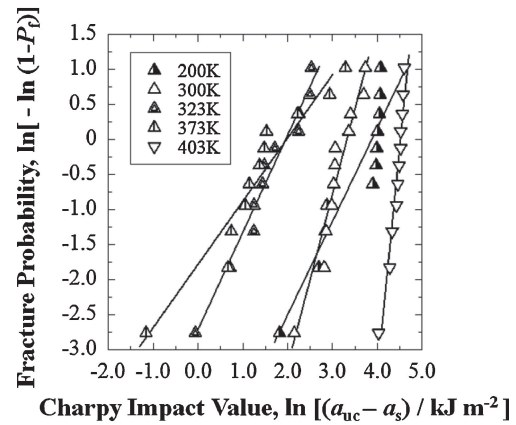


Fig. 9 Linear relationships between  $\ln(a_{uc} - a_s)$  and  $\ln[-\ln(1 - P_f)]$  for CFRP/PC/CFRP at each temperature.

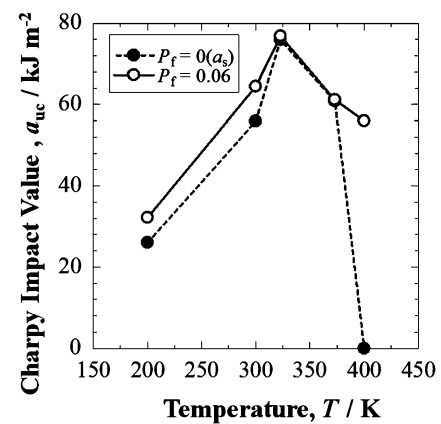


Fig. 10 Changes in experimental impact values ( $a_{uc}$ ) at low  $P_f$  of 0.06 ( $\circ$ ) and the lowest impact values ( $\bullet$ :  $a_s = a_{uc}$  at  $P_f = 0$ ) of CFRP/PC/CFRP plotted against temperature.

and 403 K, are obtained from 300 to 373 K. The highest  $a_s$  (76 kJ m<sup>-2</sup>) was found at 323 K.

#### 4.4 Impact values of CFRP/PC/CFRP at room temperature

Figure 4 also shows changes in impact value of CFRP (dotted lines) against  $P_f$  at each temperature from 200 to 403 K,<sup>15)</sup> together with CFRP/PC/CFRP (solid lines). Although the volume fraction of carbon fiber (12%) of CFRP/PC/CFRP is much smaller than that (60%) of CFRP, the  $a_{uc}$  of CFRP/PC/CFRP at room temperature (300 K) is approximately 64% higher than that of CFRP sheet at 300 K. This is caused by not only high impact value (84 kJ m<sup>-2</sup>) of PC, but could probably also occur in aviation parts during flight by microcrack toughening under load. Although the fracture cannot be observed in the PC core at testing temperature of 300 K (see Fig. 5), the delamination occurs at interface between PC core and both CFRP thin sheets to relax the impact force instead of the simple fracture of CFRP.<sup>4)</sup>

#### 4.5 Impact values of CFRP/PC/CFRP at low temperatures of 77 to 200 K

The surface CFRP delamination occurs in the CFRP/PC/CFRP cooled at nitrogen boiling point of 77 K before impact test. The linear coefficient of thermal expansion (CTE) values of PC, epoxy resins and typical carbon fiber (PAN M40) are

$66 \times 10^{-6}/\text{K}$ ,<sup>28)</sup>  $44\text{--}90 \times 10^{-6}/\text{K}$ <sup>28)</sup> and  $-1.2 \times 10^{-6}/\text{K}$ ,<sup>29)</sup> respectively. With the large CTE difference between PC core and the CFRP surface thin ply, the delamination fracture at 200 K is easily caused by the thermal expansion difference, as well as impact force.

The cooling reduces the volume of epoxy resin, whereas the CTE of carbon fiber is small. Thus, the compressive stress on the carbon fiber from epoxy resin occurs at the interface and prevents fiber pullout, resulting in enhancement of impact value of CFRP.

At 200 K (see Fig. 4), the higher  $a_{uc}$  of CFRP/PC/CFRP is found from 77 to 83  $\text{kJ m}^{-2}$  at  $P_f > 0.40$  and is higher than that of CFRP. This can be explained by fracture not being observed in the PC core at high  $a_{uc}$  at 200 K.

On the other hand, although the lower  $a_{uc}$  of CFRP/PC/CFRP at 200 K is distributed from 32 to 42  $\text{kJ m}^{-2}$  at  $P_f < 0.40$ , they are approximately equal to that of simple fractured CFRP at 200 K.<sup>4)</sup> Since the delamination is the simple dominant factor to fracture the samples at 200 K and easily occurs (see Fig. 5), the impact force is relaxed thus, it can be explained.

#### 4.6 Impact values of CFRP/PC/CFRP at high temperature

The  $a_{uc}$  of CFRP/PC/CFRP heated at 403 K, which is mostly higher than that at higher  $P_f$  values from 0.12 to 0.94 at 300 K, is also higher than that at lower  $P_f$  of less than 0.6 of CFRP at 403 K.

As shown in Fig. 5, the PC core bending and small delamination area as well as the CFRP thin sheet fracture at tensile surface side occur in the sample heated at 403 K. Since the heating near glass transition temperature of epoxy resin ( $T_g = 398 \text{ K}$ )<sup>22)</sup> enhances the fluidity, it easily relaxes the impact force by energy loss of polymer deformation. Thus, the high impact value induced by heating is explained, as shown in Fig. 4. The  $a_{uc}$  of CFRP/PC/CFRP heated at the water boiling point of 373 K, which is always lower than that at 300 K at each  $P_f$  value from 0.06 to 0.94, is always higher than that of the CFRP at 373 K. When the heating reduces the elasticity and compressive stress to prevent the pull-out, it probably reduces the resistance to deformation, resulting in the impact value drop. As shown in Fig. 5, the PC core bending and broad area peeling as well as the CFRP thin sheet fracture at the impacted surface side occurs in the sample heated at 373 K. Although the  $a_{uc}$  at 373 K of CFRP/PC/CFRP is always higher than that of CFRP, the lower impact value induced by heating at 373 K is explained, as shown in Fig. 4.

Moreover, the  $a_{uc}$  of CFRP/PC/CFRP heated at 323 K, which is mostly higher than that at 300 K at lower  $P_f$  values from 0.06 to 0.78, is always higher than that of CFRP at 323 K. The PC core undergoes bending with delamination on the tensile-side CFRP thin sheet at testing temperature of 323 K (see Fig. 5) to relax the impact force instead of the simple fracture of CFRP.<sup>15)</sup>

#### 4.7 Temperature dependent impact value of CFRP/PC/CFRP

Figure 11 shows changes in Charpy impact value of the sandwich structure CFRP/PC/CFRP at low, mid- and high

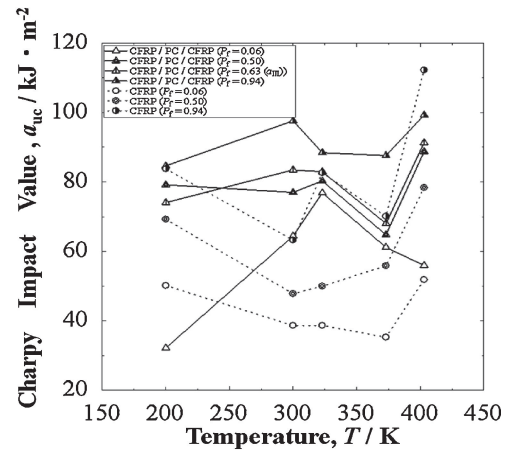


Fig. 11 Changes in Charpy impact values of CFRP/PC/CFRP at low, mid- and high  $P_f$  of 0.06, 0.5 and 0.94 against each testing temperature, together with CFRP samples.

$P_f$  of 0.06, 0.5 and 0.94 against each testing temperature, together with CFRP samples. Note the  $a_{uc}$  values of the CFRP/PC/CFRP ( $74 \pm 11 \text{ kJ m}^{-2}$  at mid- $P_f$  of 0.50 from  $T = 200$  to 403 K) are higher than those ( $57 \pm 11 \text{ kJ m}^{-2}$ ) of the CFRP. The  $a_{uc}$  values of  $55 \pm 23$  and  $92 \pm 8 \text{ kJ m}^{-2}$  at low and high  $P_f$  of 0.06 and 0.94, respectively from  $T = 200$  to 403 K of CFRP/PC/CFRP are also higher than those ( $43 \pm 10$  and  $87 \pm 25 \text{ kJ m}^{-2}$ ) of the CFRP. The higher  $a_{uc}$  at RT and mid- $P_f$  of 0.5 of CFRP/PC/CFRP can be mainly explained by the high  $a_{uc}$  of PC ( $84 \text{ kJ m}^{-2}$ )<sup>18)</sup> rather than that of CFRP ( $40 \text{ kJ m}^{-2}$ ).

Moreover, the  $a_{III}$  values at 403 K are higher than those at room temperature (300 K).

In addition, at the time of this study the cost of CFRP/PC/CFRP was 40% lower than that of CFRP. Since the use of PC resin as the core enhanced the safety design with low cost, the sandwich structural composites of CFRP/PC/CFRP can be mostly used for daily articles.

## 5. Conclusions

Impact values ( $a_{uc}$ ) of sandwich structural composites (CFRP/PC/CFRP) of polycarbonate (PC) cores covered with one ply sheets of carbon fiber cross textile reinforced epoxy (CFRP) at both side surfaces were obtained at different temperatures from 200 to 403 K below the glass transition temperature of PC. The  $a_{uc}$  of CFRP/PC/CFRP were compared with a 2.0 mm thick 12-ply CFRP laminate. Fracture mode was characterized by delamination between PC core and the surface CFRP thin sheets, bending plastic deformation of the PC, and fracture of the CFRP ply.

- (1) Results showed overall, the CFRP/PC/CFRP had higher  $a_{uc}$  than the CFRP at each fracture probability ( $P_f$ ) from 300 to 373 K except at 200 K with low  $P_f$  and 403 K with high  $P_f$ . Although the volume fraction of carbon fiber (12%) of CFRP/PC/CFRP was much smaller than that (60%) of CFRP, the  $a_{uc}$  of CFRP/PC/CFRP at room temperature (300 K) was approximately 64% higher than that of CFRP sheet at 300 K. Since the fracture could not be observed in the PC core at testing temperature of 300 K, the peeling occurred at the

interface between PC core and both CFRP thin sheets to relax the impact force, instead of the simple fracture of CFRP.

- (2) The  $a_{uc}$  values of CFRP/PC/CFRP at each fracture probability ( $P_f$ ) at 300 K as well as mid- $P_f$  of 0.50 at each temperature from 200 to 403 K were apparently higher than that of CFRP. Since the price of CFRP was higher than that of core PC, the cost of CFRP/PC/CFRP was 40% lower than that of CFRP at the time of this study. Also, since the use of PC resin as the core enhanced the safety design at low cost, practical use of sandwich structural composites of CFRP/PC/CFRP is possible.
- (3) When the CFRP/PC/CFRP sample was cooled at nitrogen boiling point of 77 K, delamination occurred before the impact test. Thus,  $a_{uc}$  could not be obtained at 77 K.
- (4) The higher  $a_{uc}$  of CFRP/PC/CFRP at 200 K was found from 77 to 83 kJ m<sup>-2</sup> at  $P_f > 0.40$ , whereas the lower  $a_{uc}$  of CFRP/PC/CFRP at 200 K was distributed from 32 to 42 kJ m<sup>-2</sup> at  $P_f < 0.40$  because of delamination of the CFRP thin sheets. Moreover, the  $a_{uc}$  at mid- $P_f$  values of 0.50 and 0.60 of CFRP/PC/CFRP cooled at 200 K were higher than those at 300 K. Since delamination easily occurs, the impact force was relaxed.
- (5) The  $a_{uc}$  of CFRP/PC/CFRP heated at 323 K was mostly higher than that at 300 K at lower  $P_f$  values from 0.06 to 0.78. It was always higher than that of CFRP at 323 K. The PC underwent bending with delamination on the tensile-side CFRP thin sheet at 323 K to relax the impact force.
- (6) Although the  $a_{uc}$  of CFRP/PC/CFRP heated at water boiling point of 373 K was always lower than that at 300 K at each  $P_f$  value from 0.06 to 0.94, it was always higher than that of CFRP at 373 K. When the heating reduced the elasticity and compressive stress to prevent the pull-out, it probably reduced the resistance to deformation, resulting in impact value drop.
- (7) The  $a_{uc}$  of CFRP/PC/CFRP heated at 403 K was mostly higher than that at 300 K at higher  $P_f$  values from 0.12 to 0.94 and was also higher than that of the CFRP at lower  $P_f$  of less than 0.60 at 403 K. Since the heating near glass transition temperature of epoxy resin enhanced the fluidity, it easily relaxed the impact force by energy loss of polymer deformation, resulting in the high impact value.
- (8) Based on the results and Weibull equations with two and three parameters, both Weibull coefficient ( $n$ ) and the limited impact value ( $a_s$ ) at 300 to 373 K were higher than those at 200 and 403 K. The highest  $a_s$  (76 kJ m<sup>-2</sup>) and  $n$  (22) were found at 323 K.
- (9) We do not claim the Charpy test to be a substitute for point impact followed by compression after impact (CAI). However, Charpy impact method with hammer hitting velocity of  $\sim 1.74$  ms<sup>-1</sup> could possibly be used as an inexpensive preliminary evaluation to screen candidate materials to later test with indentation or projectile followed by CAI. Up to now, there has been no or very little research on Charpy impact value ( $a_{uc}$ ) of composite sandwich structures. Hence, Charpy may

give a rough or better estimation of which materials and what temperatures a projectile such as bird strike, volcanic rock or hailstone will cause the most damage.

## Acknowledgement

We would like to extend our sincere gratitude to Mr. Yoshihide Ebihara M.S., Dr. Masae Kanda, and Dr. Keisuke Iwata for their great assistance.

## REFERENCES

- 1) D. K. Thomas: *Plastics Rubber Int.* **8** (1983) 53–57.
- 2) M. B. Dowell: *Plastics Eng.* **33** (1977) 31–32.
- 3) ASTM D 6264-98 (1998).
- 4) K. Imielińska, L. Guillaumat, R. Wojtyra and M. Castaings: *Compos. Part B* **39** (2008) 1034–1041.
- 5) A. S. Vaidya, U. K. Vaidya and N. Uddin: *Mater. Sci. Eng. A* **472** (2008) 52–58.
- 6) O. S. David-West, D. H. Nash and W. M. Banks: *Compos. Struct.* **83** (2008) 247–258.
- 7) L. Aktay, A. F. Johnson and M. Holzapfel: *Comput. Mater. Sci.* **32** (2005) 252–260.
- 8) K. Komai, K. Minoshima, K. Tanaka and K. Nakaie: 12th Int. Conference on Composite Materials, Paris, (1999) paper 1286, pp. 1–10.
- 9) M. Aktaş, R. Karakuzu and Y. Arman: *Compos. Struct.* **89** (2009) 77–82.
- 10) H. M. Wen, T. Y. Reddy, S. R. Reid and P. D. Shoden: *Key Eng. Mater.* **141–143** (1998) 501–552.
- 11) S.-L. Gao and J.-K. Kim: *Compos. Part A Appl. Sci. Manuf.* **32** (2001) 775–785.
- 12) V. Kostopoulos, A. Baltopoulos, P. Karapappas, A. Vavouliotis and A. Paipetis: *Compos. Sci. Tech.* **70** (2010) 553–563.
- 13) J. D. Splett, H. K. Iyer, C.-M. Wang and C. N. McCowan: *National Institute of Standards and Technology (NIST) Recommended Practice Guide*, Computing Uncertainty for Charpy Impact Test Machine Test Results; Special publication 960-18, US Department of Commerce: Boulder, Colorado (2008) pp. 27–29.
- 14) T. Yamamoto, S. Nanba, Y. Ebihara and Y. Nishi: *J. Jpn. Inst. Metals* **74** (2010) 127–130.
- 15) Y. Nishi, N. Tsuchikura, S. Nanba, T. Yamamoto and K. Iwata: submitted.
- 16) Q. Lin and A. F. Yee: *J. Mater. Sci.* **32** (1997) 3961–3970.
- 17) *Macmillan's Chemical and Physical Data*, Arthur M. James & Mary P. Lord (1986) pp. 398–399.
- 18) M. Baucio (Ed.): *ASM Engineered Materials Reference Book*, 2nd Edition, (Materials Park, Ohio: ASM International, 1994) p. 410.
- 19) J. M. Pérez, J. L. Vilas, J. M. Laza, S. Arnáiz, F. Mijangos, E. Bilbao, M. Rodríguez and L.M. León: *J. Mater. Process. Technol.* **210** (2010) 727–733.
- 20) Japanese Industrial Standards Committee: JIS K7077 (1991).
- 21) P. M. Schubel, J.-J. Luo and I. M. Daniel: *Compos. Part A Appl. Sci. Manuf.* **38** (2007) 1051–1057.
- 22) Y. Nishi, K. Inoue and M. Salvia: *Mater. Trans.* **47** (2006) 2846–2851.
- 23) Y. Nishi, H. Takei, K. Iwata, A. Vautrin and M. Salvia: *Mater. Trans.* **50** (2009) 2826–2832.
- 24) H. Takei, K. Iwata, M. Salvia, A. Vautrin and Y. Nishi: *Mater. Trans.* **51** (2010) 2259–2265.
- 25) Y. Nishi, H. Kobayashi and M. Salvia: *Mater. Trans.* **48** (2007) 1924–1927.
- 26) W. Weibull: *Ingeniörs vetenskaps akademien*, nr. 151 (Generalstabens litografiska anstalts förlag, Stockholm, 1939) pp. 12–14.
- 27) W. Weibull: *Ingeniörs vetenskaps akademien*, nr. 153 (Generalstabens litografiska anstalts förlag, Stockholm, 1939) pp. 16–22.
- 28) A. M. James and M. P. Lord: *Macmillan's Chemical and Physical Data*, London and Basingstoke, (The Macmillan Press, Ltd. 1992) pp. 398–399.
- 29) Y. Zhang and G. Wu: *Trans. Nonferrous Met. Soc. China* **20** (2010) 2148–2151.